Thermal analysis in oxidative and pyrolysis conditions of alkaline earth metals picolinates using the techniques: TG-DSC, DSC, MWTA, HSM and EGA (TG-DSC-FTIR and HSM-MS)

A.L.C.S. Nascimento[a,b], G.M.B. Parkes[b], G.P. Ashton[b], R.P. Fernandes[a], J.A. Teixeira[a], W.D.G. Nunes[a], M. Ionashiro[a, 1], F.J. Caires[a,c]

[a] *Instituto de Química, Universidade Estadual Paulista, CP 355, 14801-970 Araraquara, SP, Brazil*

[b] *Thermal Methods Research Unit, Department of Chemistry, University of Huddersfield, Queensgate, Huddersfield HD1 3DH, United Kingdom*

[c] *Faculdade de Ciências , UNESP—Univ., Estadual Paulista, Campus Bauru, Departamento de Química, Bauru, SP 17033-260, Brazil*

ABSTRACT

Synthesis, characterization, thermal stability and pyrolysis of some alkaline earth picolinates $M(C_6H_5NO_2)_2{\cdot}nH_2O$ (where M = Mg(II), Ca(II), Sr(II) and Ba(II) and n = di (Mg), mono (Ca), hemi three (Sr) hydrated) were investigated using a range of techniques including simultaneous thermogravimetry and differential scanning calorimetry (TG–DSC), evolved gas analysis (EGA), differential scanning calorimetry (DSC), Hot-Stage microscopy (HSM), powder X-ray diffractometry (PXRD), complexometry with EDTA and elemental analysis (EA). The TG-DSC curves show that the hydrated compounds dehydrate in a single step of mass loss and the thermal stability of the anhydrous compound is little influenced from the atmosphere used. On the other hand, the mechanisms of thermal decomposition are profoundly influenced by the atmosphere used, as can also be observed in the EGA data. In addition, a comparison between two calorimetric techniques, Microwave Thermal Analysis (MWTA) and DSC, was made which showed similar profiles. Two evolved gas analysis (EGA) techniques: TG-DSC coupled to FTIR and HSM coupled to a quadrupole mass spectrometer (MS) were also used to provide additional information about the pyrolysis mechanism.

Keywords: Alkaline earth picolinates; Microwave Thermal Analysis (MWTA); TG-DSC-FTIR; HSM-MS.

1. INTRODUCTION

2-Pyridinecarboxylic acid, also known as picolinic acid, has a six-membered ring structure with two active groups: a carboxylic in the ortho-position to the nitrogen in the pyridine ring, therefore, the potential donor sites leads to a variety of ligation modes [1]. Picolinic acid is a natural compound that

[1] **Corresponding author.**
e-mail address: massaoi@yahoo.com.br

exhibits chelating properties which facilitates the absorption of minerals such as: chromium, zinc, magnesium, copper, iron, and probably molybdenum [2-3]. Picolinates have been reported to possess a variety of therapeutic properties including neuroprotection, immunology, and anti-proliferative effects on the body [4–8]. Selective complexation of metal ions is also an important requirement for the use of metal complexes finding a range of applications within medicine. Indeed, chronic intoxication with a range of metal ions can be treated with the administration of a suitable chelating agent [9-11].

The literature reports studies with picolinic N-oxide forming bivalent transition metals ions [12], trivalent lanthanide ions [13–15], rare earth picolinate complexes [16-17] and others lanthanide complexes [18]. Previous papers demonstrating the thermal behavior of lanthanides picolinates have been reported [14,17], however, no systematic study about the thermal behavior of the alkaline earth metal picolinates has been found.

Microwave heating is dependent on a parameter, tan δ, which is dependent on the dielectric properties of the sample and is key to how well a material can convert electromagnetic energy into heat. Microwave Thermal Analysis (MWTA) uses microwave energy as a means of simultaneously heating a sample and detecting thermal transitions (phase changes, decomposition, etc.) through changes in the tan δ of a sample. MWTA is most often used in a differential temperature configuration [19] where the difference between the sample and an inert reference (SiC) is recorded. If a sample undergoes enthalpic changes but no significant changes in tan δ then the trace produced approximates that seen with a DTA/DSC. However, if the sample undergoes a change that affects tan δ this is shown as steps on the differential temperature trace. For certain systems, MWTA has the potential for greater sensitivity than conventional DSC but this is very sample dependent [20].

In recent years microwave heating has been used for processing and drying of chemicals [21-23]. The suitability of the method for the drying of pharmaceuticals has been extensively investigated [24], for example, with the application for maintenance of drug stability [25]. To date, MWTA has only been applied to simple metal salts and hydrates and not more complex compounds such as picolinates.

The present paper aims to investigate the thermal behavior of picolinic acid and its compounds with some alkaline earth ions: $Mg(C_6H_4NO_2)_2{\cdot}2H_2O$, $Ca(C_6H_4NO_2)_2{\cdot}H_2O$, $Sr(C_6H_4NO_2)_2{\cdot}1.5H_2O$ and $Ba(C_6H_4NO_2)_2$. The characterization was performed using thermoanalytical techniques (TG-DSC, DSC, MWTA, and HSM) and complementary techniques such as PXRD. A comparison has been made between hyphenated techniques to evaluate gaseous decomposition products of metal picolinates through EGA using TG-DSC-FTIR and HSM-MS.

2. Experimental

2.1. Chemicals

Picolinic acid (99% purity) was obtained from Sigma and was used as received. The calcium, strontium and barium carbonates were obtained from Fluka (Ca, 99.5%), Merck (Sr, Ba, 99% purity) and magnesium carbonate was prepared as described in reference [28].

2.2.Preparation

Solid-state alkaline earth metal picolinates (Mg to Ba) were synthesized following methodology previously reported [28].

2.3.Experimental equipment and conditions

The composition of the compounds was determined by elemental analysis (CHN Elemental Analyzer from Perkin Elmer, model 2400), TG data and EDTA complexometry [26, 27].

Simultaneous TG-DSC curves were obtained by using a TG–DSC 1 STAR^e system, from Mettler Toledo and according to the methodology described in reference [14]. The purge gas used was either dry air or nitrogen with a flow rate of 50 mL min^{-1} and a heating rate of 10 ° C min^{-1}, and samples weighing approximately 10 mg in open alumina crucibles.

The DSC curves were obtained by using DSC STAR^e system, from Metter Toledo. The purge gas was nitrogen with a flow rate of 100 mL min^{-1}. A heating rate of 10 °C min^{-1} was adopted, with samples weighing about 3 mg placed in aluminum crucibles with a perforated lid.

The identification of evolved gases (EGA) in dynamic dry nitrogen atmosphere were carried out using a TG-DSC 1 Mettler Toledo coupled to a Nicolet FTIR spectrophotometer with gas cell and DTGS KBr detector using the method described in reference [29]. The furnace and heated gas cell (250 °C) were coupled through a heated (225 ˚C) 120 cm stainless steel transfer line with diameter of 3.0 mm, both purged with dry air and nitrogen (50 mL min^{-1}). The FTIR spectra were recorded with 16 scans per spectrum at a resolution of 4 cm.

Hot-stage microscopy (HSM) measurements were performed using a system developed at Huddersfield [30] which utilizes a stereoscopic microscope (Leica) and a water cooled hot-stage (HSM5, Stanton-Redcroft). Samples were placed in 5-6 mm alumina crucibles using sample masses of 10 mg, linear heating rates of 10 °C min^{-1} under an inert atmosphere. Micrographs were recorded every 5 °C.

The HSM system was coupled to a quadrupole mass spectrometer (HPR20, Hiden, Warrington, UK). Evolved sample gases were transferred via a heated capillary line to the inlet of the spectrometer, full mass scans were recorded between 4 and 300 mass units with an accumulation time of 200 ms per scan.

Microwave thermal analysis was performed using an instrument previously developed at Huddersfield [19]. The system utilizes a 300 W 2.45 GHz generator (Sairem) and a single mode waveguide. The generator is computer controlled with a power resolution corresponding to 1W. The standing wave is

tuned to achieve the maximum of the E-field over the position of the sample. Samples of 40 mg were placed within silica crucibles (fundamentally microwave transparent) and heated at a rate of 10 °C min^{-1} up to an upper temperature of 450 °C. DTA microwave measurements are made between the sample and a reference of silicon carbide.

Powder X-Ray Diffraction (PXRD) patterns analyses were obtained using a Bruker D2 Phaser employing CuKα radiation (λ = 1.5418 Å) and settings of 30 KV and 10 mA. The analysis were performed in an angular range from 5 - 80 º (2θ), scanning speed 0.5 seconds, and 0.02º steps.

3. Results and discussions

3.1. Analytical results

The analytical results (TG, EA and EDTA complexometry) of the synthesized compounds are shown in Table 1. These results are in close agreement with each other and with the calculated theoretical values, which shows that the compounds were obtained with excellent purity. In addition, from these results it was possible to determine the empirical formula of these compounds, which is in agreement with the general formula: $M(L)_2 \cdot nH_2O$, where M represents Mg, Ca, Sr and Ba, L is picolinate and n = 2 (Mg), 1 (Ca), 1.5 (Sr) and 0 (Ba).

Insert Table 1

3.2.Thermal Analysis

The simultaneous enthalpy and mass loss curves from TG-DSC curves in dynamic dry air and nitrogen atmospheres are shown in Fig.1 (a-d) and (a*-d*), respectively. In an air atmosphere, these curves exhibit mass losses in either a single (Ba), three (Mg, Sr) or four (Ca) steps. While for nitrogen three (Mg, Sr, Ba) and four (Ca) steps were observed.

Thermal decomposition of the picolinate compounds in an oxidative atmosphere was monitored up to 1000°C, the final residues for Mg, Ca and Sr were the respective oxides and carbonate for barium. In contrast, the pyrolytic atmosphere (N_2) shows gradual mass losses that are still apparent up to 1000 °C for Mg, Sr and Ba (forming a mixture of respective oxides and charred material) with only Ca picolinate forming its oxide within this temperature range.

The TG-DSC profiles of the compounds in air atmosphere are not the same in N_2, thus these curves in each atmosphere are discussed separately below.

The DSC and MWTA provided information necessary for identification of the physical phenomena of melting (Mg, Ca), glass transitions (Mg, Ca), and phase transitions (Ba, Ca). The dehydration of all the compounds, except barium, is more clearly observed using DSC rather than simultaneous TG-DSC data.

3.2.1. TG-DSC under an air atmosphere

The simultaneous TG-DSC curves of the compounds in an air atmosphere are shown in Fig. 1 (a-d). The TG curve shows that the barium compound was obtained as anhydrous, while calcium compound as mono-hydrate, strontium and magnesium as hemi-three and di-hydrated, respectively. These curves also show that the dehydration in all the compounds (except barium) occurs in a single step. The thermal stability of the hydrated compounds, as well as the final temperature of thermal decomposition to the respective oxides as shown by TG-DSC curves, depends on the nature of the metal ion and follow the order:

Dehydration stability: Mg > Ca > Sr

Decompoition stability: Ba > Sr > Ca = Mg

The thermal behavior of the compounds is also dependent on the nature of the metal ion and so the features of each of these compounds are discussed individually.

Magnesium picolinate

The simultaneous TG-DSC curves are shown in Fig.1 (a). The first mass loss between 50 and 175 ºC, with a corresponding endothermic peak at 148 ºC is attributed to the dehydration with loss of 2 H_2O ($\Delta m_{calc.}$ = 11.76%, Δm_{TG} = 12.27%). The anhydrous compound is stable up to 390 ºC. Above this temperature the mass losses occurs in two overlapping steps between 390-415 ºC (Δm_{TG} = 35.07%) and 415-550 ºC (Δm_{TG} = 39.26%), corresponding to an endothermic peak at 408 ºC and is attributed to the beginning of thermal decomposition. An exothermic peak at 490 ºC, with shoulder at 460 ºC is attributed to the thermal decomposition and oxidation of the organic matter and/or the gaseous products evolved during the thermal decomposition, respectively. The total mass loss up to 535 ºC is in agreement with the formation of magnesium oxide (MgO), as the final residue ($\Delta m_{calc.}$ = 86.61%, Δm_{TG} = 86.85%).

The small endothermic peak at 398 ºC, at the beginning of the mass loss is due to the melting of the compound as discussed in the DSC and MWTA sections.

Calcium picolinate

The simultaneous TG-DSC curves are shown in Fig 1 (b). The first mass loss up to 170 ºC, corresponding to an endothermic peak at 145 ºC and is attributed to the dehydration with loss of H_2O ($\Delta m_{calc.}$ = 5.92%, Δm_{TG} = 6.23%).

The anhydrous compound is stable up to 390 ºC and above this temperature the thermal decomposition occurs in three consecutive steps, with the first two overlapping. The two overlapping mass loss steps observed between 390-460 ºC (Δm_{TG} = 35.89%) and 460-515 ºC (Δm_{TG} = 23.95%) have an

exothermic peak centred at 460 ºC. These changes are attributed to oxidation of the organic matter and/or the loss of gaseous products evolved during the thermal decomposition. The total mass loss up to 515 ºC is in agreement with the formation of calcium carbonate as a residue ($\Delta m_{calc.}$ = 66.89%, Δm_{TG} = 66.91%) which is stable until about 570 °C.

The final mass loss step observed between 570 ºC and 700 ºC (Δm_{TG} = 14.75%), is attributed to the thermal decomposition of the carbonate to the calcium oxide as a final residue ($\Delta m_{calc.}$ = 14.56%, Δm_{TG} = 14.43%). The total mass loss up to 670 ºC is in agreement with the formation of calcium oxide, CaO, as final residue (Calcd. = 81.59%, TG = 81.55%).

The very small exothermic peak at 275 ºC and the endothermic peak at 360 ºC (both not associated with a mass loss from the TG curve) are attributed to crystallization process and melting of the compound. These processes were more apparent HSM, DSC and MWTA as discussed latter.

Strontium picolinate

The simultaneous TG-DSC curves are shown in Fig. 1 (c). A gradual mass loss is observed up to 300 ºC, although no events on the DSC curve are apparent. To evaluate this mass loss, the sample was heated in a glass tube up to 300 °C for 15 min where evaporation followed by condensation was observed. The residue condensed on the wall of the tube was analyzed using FTIR which confirmed that water was evolved. Therefore the gradual mass loss was attributed to dehydration with loss of $1.5H_2O$ ($\Delta m_{calc.}$ = 7.49%, Δm_{TG} = 7.11%).

The anhydrous compound remained stable up to 415 ºC but above this temperature mass loss occurs through a fast process corresponding to a large and sharp exothermic peak at 450 ºC. This mass change is attributed to thermal decomposition and oxidation of the organic matter. The mass loss up to 500 ºC is in agreement with the formation of strontium carbonate as residue ($\Delta m_{calc.}$ = 55.51%, Δm_{TG} = 55.43%), which is stable up to 790 ºC.

The last mass loss occurs between 790 ºC and 940 ºC is attributed to the thermal decomposition of the carbonate to the strontium oxide SrO, as final residue ($\Delta m_{calc.}$ = 11.40%, Δm_{TG} = 12.04%).

Barium picolinate

The simultaneous TG-DSC curves are shown in Fig 1 (d). The anhydrous compound is stable up to 400 ºC and above this temperature the thermal decomposition occurs through a fast process corresponding to a large and a sharp exothermic peak at 475 ºC with shoulder at 440 ºC. These changes are attributed to oxidation of the organic matter and/or the loss of gaseous products evolved during the thermal decomposition. The mass loss up to 500 ºC is in agreement with the formation of barium carbonate as

residue ($\Delta m_{calc.}$ = 50.27%, Δm_{TG} = 50.66%). The barium carbonate, $BaCO_3$, formed is stable to 920 ºC but above this temperature begins further decomposition which has not completed by 1000 ºC.

The very small endothermic peaks at 211 ºC and 780 ºC, (both not associated with a mass loss from the TG curve) , have been tentatively assigned to crystalline phase transition (corresponding to the endothermic peak on DSC curve at 241 ºC, see in Figure 4) and phase transformation (α-β) of the barium carbonate, respectively.

Insert Figure 1

3.2.2. TG-DSC – N_2 atmosphere

The simultaneous TG and DSC curves of the compounds are shown in Fig. 1 (a*-d*). These curves show mass losses in consecutive steps and endothermic peaks corresponding to the losses or due to physical phenomenon.

The thermal stability of the hydrated and anhydrous compounds depends on the nature of the metal ion and they follow the order:

Dehydration stability: Ca > Mg > Sr

Decomposition stability: Ba > Sr > Ca = Mg

For all hydrated compounds, the dehydration step is, as expected, very similar to that observed in the oxidizing atmosphere. However, a significant difference is observed in the thermal decomposition of these compounds, suggesting a strong influence of the atmosphere. The final temperature of the thermal decomposition is observed only for the calcium compound, for the other compounds the mass loss is incomplete by 1000 ºC.

As previously observed in an air atmosphere, and as will be shown for a N_2 one, the thermal behavior also depends on the nature of the metal ion, features of each of these compounds are discussed individually.

<u>Magnesium picolinate</u>

The simultaneous TG-DSC curves are shown in Fig. 1 (a*). The first step between 50 ºC and 170 ºC, corresponding to an endothermic peak at 165 ºC is attributed to dehydration with loss of $2H_2O$ in the same way as the oxidative atmosphere ($\Delta m_{calc.}$ = 11.83%, Δm_{TG} = 11.42%). The anhydrous compound is stable up to 385 ºC and above this temperature the thermal decomposition occurs in two consecutive steps, a sharp step between 385-490 ºC (Δm_{TG} = 42.34%) and a slow mass loss starting 490 ºC (Δm_{TG} = 27.78%) which correspond to small, broad endothermic peaks at 450 ºC and 950 ºC. These steps have been attributed to the thermal decomposition and incomplete pyrolysis of the compound. The endothermic peak at 390 ºC has been attributed to the melting of the magnesium compound.

Calcium picolinate

The simultaneous TG-DSC curves are shown in Fig. 1 (b*). The first mass loss with a corresponding endothermic peak at 175 ºC is attributed to the dehydration which, again, shows similarities to the air example ($\Delta m_{calc.}$ = 5.96%, Δm_{TG} = 5.83%).

The anhydrous compound remains stable up to 390 ºC and above this temperature the thermal decomposition occurs in three consecutive steps between 390-520 ºC (Δm_{TG} = 46.68%), 520-740 ºC (Δm_{TG} = 20.57%) and 740-920 ºC (Δm_{TG} = 9.40%), corresponding to endothermic peaks at 415 ºC, 425 ºC, 435 ºC, 730 ºC and 845 ºC, the first step is attributed to the thermal decomposition of the compound with formation of calcium carbonate and carbonized residue and the last two steps to the pyrolysis of the carbonized residue and thermal decomposition of calcium carbonate leading to calcium oxide ($\Delta m_{calc.}$ = 81.45%, Δm_{TG} = 81.48%).

The minor exothermic peak at 305 º C and the endothermic peak at 390 º C, (both not associated with a mass loss from the TG curve) are attributed to crystallization process and fusion of the compound, respectively.

Strontium picolinate

The simultaneous TG-DSC curves are shown in Fig. 1 (c*). A small broad mass loss is noted between 50 and 300 ºC which has been attributed to dehydration with loss of $1.5H_2O$ ($\Delta m_{calc.}$ = 7.49%, Δm_{TG} = 7.08%). The anhydrous compound is stable up to 420 ºC but above this temperature, the mass losses occur in three consecutive steps, between 420-550 ºC (Δm_{TG} = 36.33%), 550-800 ºC (Δm_{TG} = 25.16%) and 800-1000 ºC (Δm_{TG} = 7.17%). The first mass loss is attributed to thermal decomposition and the second one to the pyrolysis of the strontium carbonate formed and/or charred residue. However, there is some indication that the final mass loss is incomplete by 1000 °C.

Barium picolinate

The simultaneous TG-DSC curves are shown in Fig. 1 (d*). The anhydrous compound is stable up to 450 ºC but above this temperature the mass losses occur in three consecutive steps between 450-530 ºC (Δm_{TG} = 27.66%), 530-800 ºC (Δm_{TG} = 19.73%) and 800-1000 ºC (Δm_{TG} = 10.32%). The first mass loss (with an associated endotherm at 490 °C) is attributed to thermal decomposition to barium carbonate and organic residue. This occurs at a much lower temperature under nitrogen due to the absence of CO_2 in this atmosphere as was previously reported [28]. The second broad mass loss step (with an associated

endotherm at 750 °C) is attributed to pyrolysis of the residue. However, there is some indication of further mass loss which is incomplete by 1000 °C.

The endothermic peak at 245 ºC without mass loss is due to the crystalline transition of the compound (see in section 3.3, discussion about Figure 5).

3.3.Differential Scanning Calorimetry (DSC)

The DSC curves under a nitrogen atmosphere are shown in Figs. 2 to 5 together with associated HSM and PXRD data to aid the visualization of the phonomenon attributed to physical or chemical processes. This combination of data sets has provided information that expands on what the TG-DSC curves have already shown, but has helped elcucidate unresolved thermal events.

Figure 2 shows the DSC curve for the magnesium picolinate with three thermal events attributed to dehydration (endothermic peak at 200 ºC), melt (endothermic peak at 391 ºC), where the enthalpies found for the compound were -0.453 kJ g^{-1} and -0.002 kJ g^{-1}, respectively, and glass transition (midpoint at 254 ºC). PXRD analysis shows that the structure varies with heating (see insert 1 diffractogram at 25 °C and insert 2, diffractogram at 270 ºC) are significantly different from each other as above the glass transition temperature the compound becomes amorphous. Changes in the color of the compound were observed after the glass transition and also at the start of melt at 370 ºC. The slight darkening of the sample above 370 °C is attributed to be the onset of decomposition.

Insert Figure 2

Figure 3 (a) shows the DSC curve with four thermal events attributed to dehydration (endothermic peak at 188 ºC), phase transition (peak at 303 ºC), melt (peak at 388 ºC), where the enthalpies found for the compound were -0.254 kJ g^{-1}, +0.055 kJ g^{-1} and -0.096 kJ g^{-1} respectively, and a possible glass transition (midpoint at 246 ºC). The three PXRD patterns (1, 2 and 3) show a reduction in Bragg peaks as the temperature is increased attributed to the loss of crystallinity. The thermally cycled DSC experiment (Figure 3 (b)) shows that the thermal event at 303 ºC is irreversible. The micrographs show that the sample contracts between 240 °C and 275 °C which may be due to a glass transition. The final micrograph at 390 °C clearly shows the effect of melting.

Insert Figure 3

Figure 4 (a) show the DSC curve for strontium picolinate which is poorly resolved at the heating rate used. Figure 4 (b) show the cycled DSC curve using a slow heating rate (2 ºC min^{-1}) to increase resolution. An endothermic event with peak at 176 ºC was observed where the dehydration enthalpy found was -0.332 kJ g^{-1}. Neither DSC curves clearly show other thermal events. However, for confirmation, the

sample was analyzed using PXRD before and after dehydration. The PXRD patterns indicate that the compound increases in crystallinity after dehydration. Large changes in the color of the compound are shown in the HSM micrographs before and after dehydration and, unlike the other picolinates, the strontium compound starts to degrade without showing signs of melting.

Insert Figure 4

Figure 5 (a) shows the DSC curve for barium picolinate with two thermal events attributed to phase transformation (endothermic peak at 113 ºC) and crystalline transition (endothermic peak at 241 ºC), the enthalpies found were – 0,003 kJ g^{-1} and -0,016 kJ g^{-1}, respectively. For this compound, the DSC analysis was very important since phase transformation cannot be observed directly using TG-DSC curves in both atmospheres. The source of the sharp endothermic peak at 241 ºC is unassigned. Although very similar to what would be observed for melting, the HSM clearly shows that this does not occur. The cycle DSC experiment (Fig. 5b) show that the endothermic peaks at 113 ºC and 241 ºC are both reversible so it was not possible to obtain material for PXRD analysis.

Insert Figure 5

3.4. Microwave Thermal Analysis (MWTA)

Figure 6 (a-d) displays differential temperature traces obtained using MWTA for the four picolinate compounds. It should be noted that the relatively large drift in the baseline is not uncommon for this technique.

Figure 6 (a) shows the MWTA trace for magnesium picolinate. The first noticable transition is an endothermic peak around 200 °C attributed to the dehydration of the compound as also observed with DSC. Further heating yeilds a slight increase in coupling with microwave energy possibly linked to the glass transition shown in the DSC curve. The the onset of decomposition, as confirmed by TG-DSC curve, is apparent from the variation in the basline folowed by a sharp step above 400 °C. Upon cooling two main steps are seen, but are diffciult to assign because full decomposition was not achieved.

Insert Figure 6

Figure 6 (b) show the MWTA trace for calcium picolinate. The endothermic dehydration can be seen at 200 °C and is clearly observed mirroring the signal obtained by the DSC. No indication of a glass transition was observed, although the attributed crystaline phase change at 300 °C shows a corresponding

step change in tan δ. The melting/decomposition step at 380 °C is at a similar temperature to that noted on the DSC, since the calcium picolinate exists in a liquid state now the sample can be seen to couple more strongly with the microwave enegry.

The MWTA trace for strontium picolinate is shown in Figure 6 (c). Unlike the DSC, the MWTA has few features and no discrnible sign of dehydration. There is a suggestion of a change at 413 °C that could be associated with decomposition onset although this process unlikely reached completion by 450 °C.

The MWTA trace for barium picolinate is shown in Figure 6 (d). The small step change at 250 °C has been attributed to the crystaline phase change observed using DSC. The baseline does not vary significantly after this event and no significant events are seen during cooling.

3.5.Evolved Gas Analysis (EGA) of magnesium picolinate

Initial experiments using TG-DSC-FTIR showed all the four picolinates studied yielded water, carbon monoxide, carbon dioxide and pyridine (except water for barium compound which is anhydrous). The decomposition of magnesium picolinate was probed in more detail using HSM-MS. Figure 7 shows the IR spectra of the gaseous products evolved during the thermal decomposition of magnesium picolinate at 10 °C min^{-1}. Figure 7 (a) shows the Gram-Schmidt trace which gives an indication of the FTIR intensity over time with three steps evident that can be linked to the TG-DSC curves in Figure 1(a*). Figutre 7 (b) shows the FTIR spectra at 160 °C (Step1) 430 °C (Step 2). The first spectra clearly shows the water produced during dehydration while the second spectra confirms that pyridine is produced during decomposition.

Insert Figure 7

Figure 8 shows the decomposition of magesium picolinate monitored using HSM-MS with an inert atmosphere. Three gaseous compounds are plotted water (18 Da), carbon dioxide (44 Da) and pyridine (79 Da). The pyridine was confirned by monitoring of the pyridine fragment ions (26, 27, 39 and 52 Da) but these have not been shown for clarity. The results confirm those observed with TG-DSC-FTIR with water being the sole product during the dehydration and pyridine being apparent during the decomposition stage. The HSM-MS indicates that both water and carbon dioxide are released during the decomposition indicating that the process is more complex than suggested by FTIR.

Insert Figure 8

4. CONCLUSIONS

From the elemental analysis, complexometry and thermogravimetric results the stoichiometry of the compounds were determined as the having the empirical formula: $M(L)_2.nH_2O$.

The TG–DSC results provided previously unreported information about the thermal stability and thermal decomposition of these compounds under oxidative and inert atmospheres. These results show that the atmosphere used plays a significant role in the thermal decomposition process of this class of compounds, since thermal stability, thermoanalytical curves and mass loss steps are all affected.

TG-DSC-FTIR analysis of the gaseous products from magnesium picolinate demonstrates that the main decomposition proceeds with release of pyridine, CO and CO_2. The ability of HSM-MS to monitor multiple ions confirms the evolution of pyridine and suggests that thermal degradation occurs by a much more complex mechanism than suggested by TG-DSC-FTIR.

The DSC and MWTA data provided information about the physical transformation undergone by the picolinates. For these compounds the decomposition did not appear to lead to significant changes in tan δ and thus MWTA was less sensitive than DSC.

The results further demonstrate the use of powder X-ray diffractometry in the elucidation of thermal processes.

5. ACKNOWLEDGMENTS

The authors thanks University of Huddersfield, FAPESP (Proc. 2017/14936-9 and 2018/12463-9), CNPq (Proc. 421469/2016-1) and CAPES Foundations (Brazil) for financial support. This research was supported by resources supplied by PDSE from CAPES Foundation (Proc. 88881.135291/2016-01).

6. REFERENCES

[1] SOMPHON, W.; HALLER, K. J. Crystal growth and physical characterization of picolinic acid cocrystallized with dicarboxylic acids. **Journal of Crystal Growth**, v. 362, n. 1, p. 252–258, 2013.

[2] SUZUKI, K.; YASUDA, M.; YAMASAKI, K. Stability constants of picolinic and quinaldic acid chelates of bivalent metals. **Journal of Physical Chemistry**, v. 61, n. 2, p. 229–231, 1957.

[3] REBELLO, T.; LONNERDAL, B.; HURLEY, L. S. Picolinic acid in milk, pancreatic juice, and intestine: inadequate for role in zinc absorption. **American Journal of Clinical Nutrition**, v. 35, n. 1, p. 1–5, 1982.

[4] WANG, X.; DAVIS, I. *et al.* Improved separation and detection of picolinic acid and quinolinic acid by capillary electrophoresis-mass spectrometry: Application to analysis of human cerebrospinal fluid. **Journal of Chromatography A**, v. 1316, p. 147–153, 2013.

[5] SHARMA, G.; NARULA, A. K. Synthesis and optoelectronic properties of three Eu(III)-dipicolinate complexes based on α-picolinic acid, 2-aminopyridine and 2-hydroxypyridine as secondary ligands.

Journal of Materials Science: Materials in Electronics, v. 26, n. 2, p. 1009–1017, 2014.

[6] CHUANG, S. C.; FANIDI, A. *et al.* Circulating biomarkers of tryptophan and the kynurenine pathway and lung cancer risk. **Cancer Epidemiology Biomarkers and Prevention**, v. 23, n. 3, p. 461–468, 2014.

[7] YUOH, A. C. B.; AGWARA, M. O. *et al.* Synthesis, Crystal Structure and Antimicrobial Properties of an Anhydrous Copper(II) Complex of Pyridine-2-Carboxylic Acid. **International Journal of Chemistry**, v. 7, n. 1, p. 10–20, 2014.

[8] LI, D.; ZHONG, G. Synthesis , Crystal Structure , and Thermal Decomposition of the Cobalt (II) Complex with 2-Picolinic Acid. **The Scientific World Journal**,v. 2014, p. 1-7, 2014.

[9] MACKAY, D.; HATHCOCK, J.; GUARNERI, E. Niacin: chemical forms, bioavailability, and health effects. **Nutrition Reviews**, v. 70, n. 6, p. 357–366, 2012.

[10] REGUEIRO-FIGUEROA, M.; RUSCSÁK, E. *et al.* Highly Stable Complexes of Divalent Metal Ions (Mg^{2+}, Ca^{2+}, Cu^{2+}, Zn^{2+}, Cd^{2+}, and Pb^{2+}) with a Dota-Like Ligand Containing a Picolinate Pendant. **European Journal of Inorganic Chemistry**, v. 2014, n. 36, p. 6165–6173, 2014.

[11] CARLESON, L. A. Nicotinic acid: the broad-spectrum lipid drug. A 50th anniversary review, **Journal of Internal Medicine**, v. 258, n. 2, p. 94–114, 2005.

[12] BOYD, S. A.; KOHRMAN, R. E.; WEST, D. X. Transition metal ion complexes of 2-picolinate N-oxide. **Journal of Inorganic and Nuclear Chemistry**, v. 38, n. 3, p. 607–608, 1976.

[13] BOYD, S. A.; KOHRMAN, R. E.; WEST, D. X. Cationic lanthanide complexes of 2-picolinic acid n-oxide. **Inorganic Nuclear Chemistry Letters**, v. 12, n. 8, p. 603–608, 1976.

[14] DO NASCIMENTO, A. L. C. S.; TEIXEIRA, J. A. *et al.* Thermal behavior, spectroscopic study and evolved gas analysis (EGA) during pyrolysis of picolinic acid, sodium picolinate and its light trivalent lanthanide complexes in solid state. **Journal of Analytical and Applied Pyrolysis**, v. 119, p. 242-250, 2016.

[15] LIS, S.; PISKUŁA, Z.; KUBICKI, M. The structure and spectroscopy of lanthanide(III) complexes with picolinic acid N-oxide in solution and in the solid state. **Materials Chemistry and Physics**, v. 114, n. 1, p. 134–138, 2009.

[16] KECK, N. B.; HORNUNG, N. J.; BOS, W. G. The preparation and characterization of some rare earth picolinate complexes. **Journal of Inorganic and Nuclear Chemistry**, v. 36, n. 7, p. 1521–1525, 1974.

[17 MOYNE, L.; THOMAS, G. Etude thermogravimétrique des picolates et dipicolates de lanthane, praséodyme et néodyme. **Analytica chimica acta**, v. 29, p. 66–69, 1963.

[18] GOMES, D. J. C.; CAIRES, F. J. *et al.* Synthesis, characterization, thermal and spectroscopic studies of solid glycolate of light trivalent lanthanides, except promethium. **Thermochimica Acta**, v. 587, p. 33–41, 2014.

[19] Parkes, G. M. B.; Barnes, P.A. *et al.* Microwave thermal analysis - A new approach to the study of the thermal and dielectric properties of materials. **Journal of Thermal Analysis and Calorimetry**, v. 56, p. 723-731, 1999

[20] Parkes, G. M. B.; Barnes, P.A. *et al.* Development of a new instrument for performing microwave thermal analysis. **Review of Scientific Instruments**, v. 71, p. 168, 2000

[21] NMAB-473 Publication, Committee on microwave processing of materials: an emerging industrial technology. Microwave processing of materials. Washington DC, USA: National Academy Press;1994.

[22] KINGSTON, H. M.; HASWELL S. J. Microwave enhanced chemistry. Washington, USA: American Chemical Society; 1997.

[23] CHEE S, N.; JOHANSEN, A. L. *et al.* Microwave drying of granules containing a moisture sensitive drug: a promising alternative to fluid bed and hot air oven drying. **Chemical and Pharmaceutical Bulletin**, v. 53, n. 7, p. 770-775, 2005.

[24] LOH, Z. H.; LIEW, C. V. *et al.* Microwave-assisted drying of pharmaceutical granules and its impact on drug stability. **International Journal of Pharmaceutics**, v. 359, n. 1-2, p.53-62, 2008.

[25] MONEGHINI, M.; ZINGONE G.; DE ZORDI, N. Influence of the microwave technology on the physical–chemical properties of solid dispersion with nimesulide. **Powder Technolology**, v. 195, n. 3, p. 259-63, 2009.

[26] FLASCHKA, H. A. EDTA Titrations and Introduction to Theory and Practice, 2nd ed., Press Oxford, Pergamon, 1964.

[27] IONASHIRO, M.; GRAMER, C. A. F.; ZUANON NETTO, J. Titulação complexométrica de lantanideos e ítrio. **Eclética Química**, v. 8, n. 1, p. 29-32, 1983.

[28] NASCIMENTO, A. L. C. S.; CAIRES, F. J. *et al.* Thermal study and characterization of nicotinates of some alkaline earth metals using TG–DSC–FTIR and DSC-system photovisual. **Thermochimica Acta**, v. 604, p. 7-15, 2015.

[29] TEIXEIRA, J. A.; NUNES, W. D. G. *et. al.* Thermal behavior in oxidative and pyrolysis conditions and characterization of some metal p-aminobenzoate compounds using TG–DTA, EGA and DSC-photovisual system. **Journal of Analytical and Applied Pyrolysis**, v. 128, p. 261-267, 2017.

[30] Berger, B.; Brammer, A. J. *et al.* Thermomicroscopy studies on the zirconium-potassium perchlorate-nitrocellulose pyrotechnic system. **Thermochimica Acta.** v. 269/270, p. 639-648, 1995.

Figures

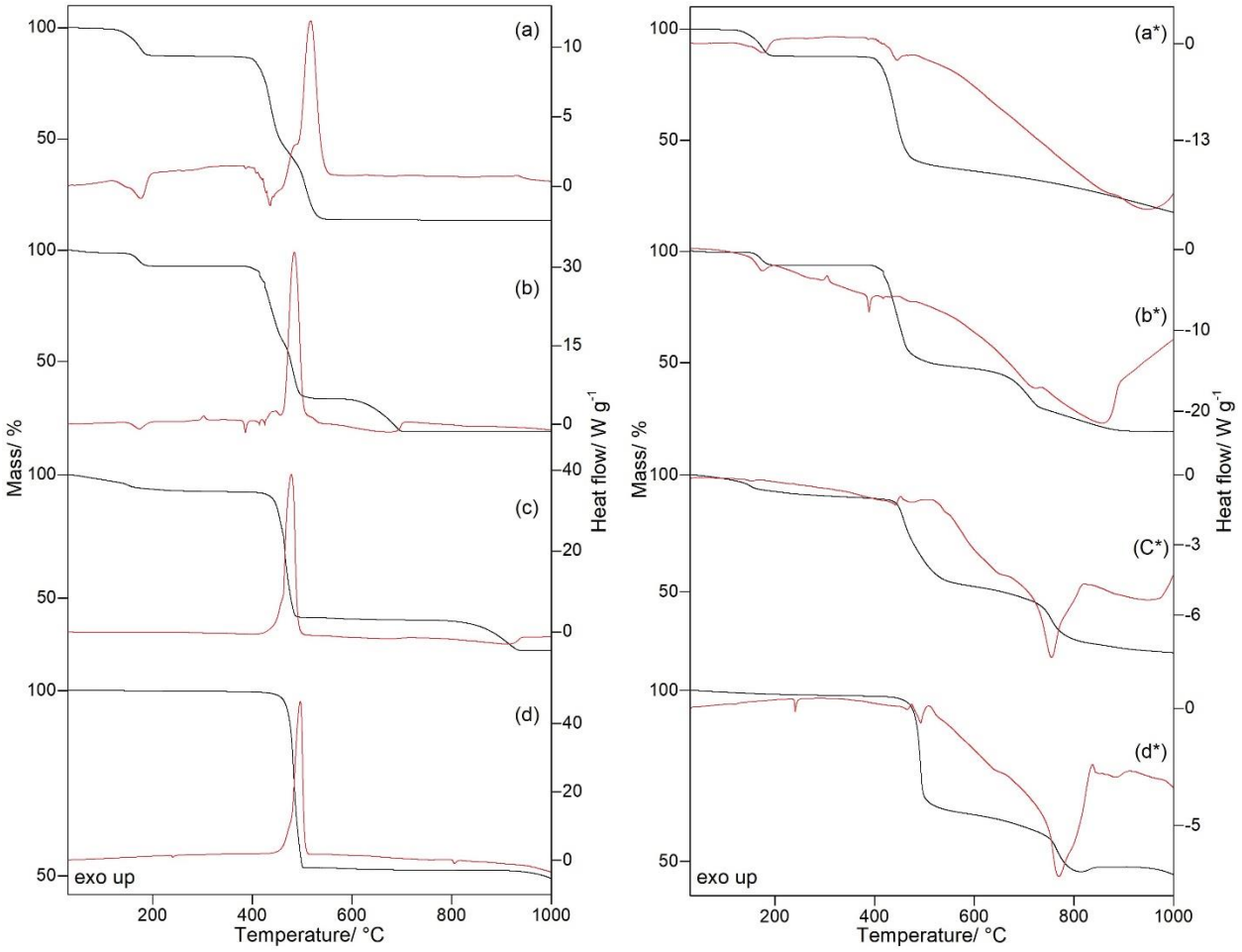

469

470 Figure 1: TG-DSC curves in air (a-d) and nitrogen (a*-d*) atmospheres of the compounds, where (a and
471 a*) represents Mg; (b and b*) represents Ca; (c and c*) represents Sr and (d and d*) represents Ba.

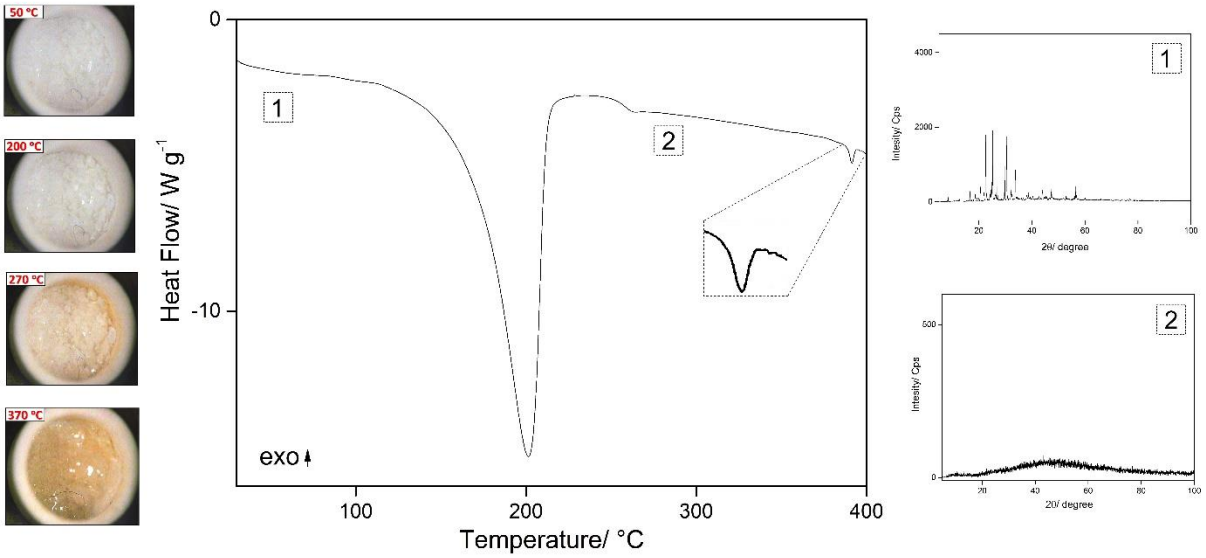

472

473 Figure 2: DSC curve, HSM micrographs and PXRD of magnesium picolinate.

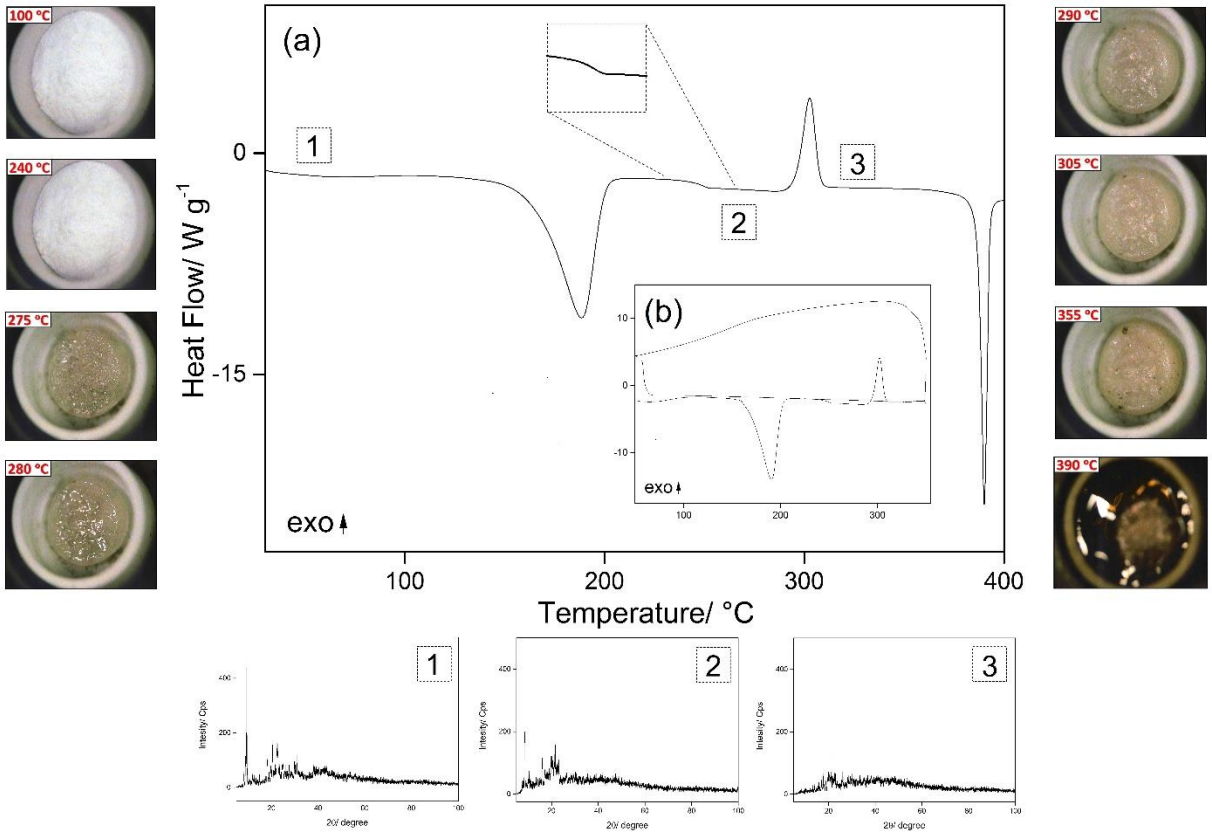

474

475 Figure 3: DSC curve (a), thermally cycled DSC experiment (b), HSM micrographs and PXRD of calcium
476 picolinate.

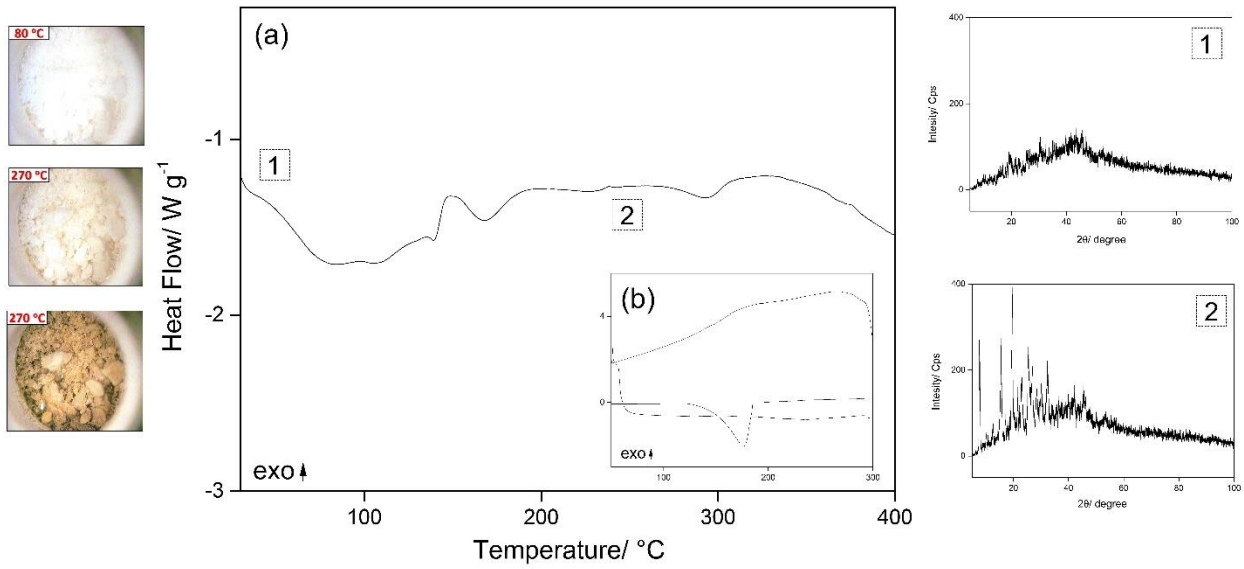

477

478 Figure 4: DSC curve (a), thermally cycled DSC experiment (b), HSM micrographs and PXRD of strontium
479 picolinate.

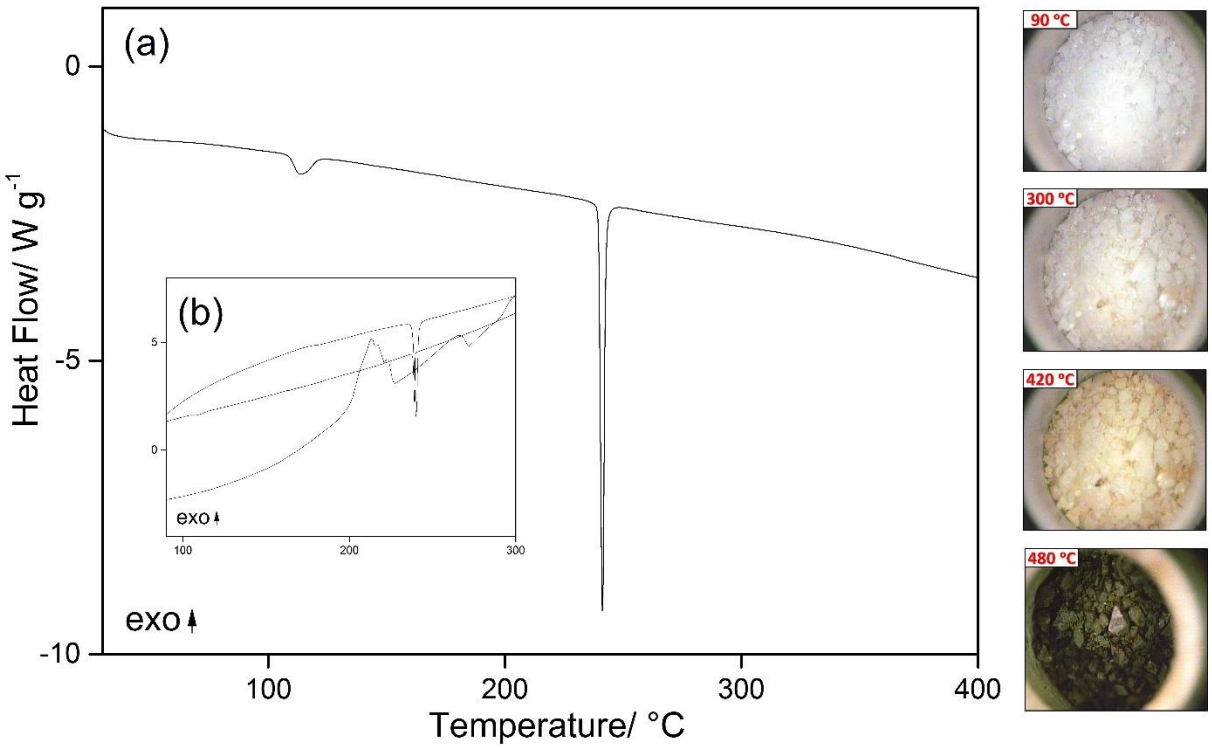

480

481 Figure 5: DSC curve (a), thermally cycled DSC experiment (b) and HSM micrographs of barium picolinate.

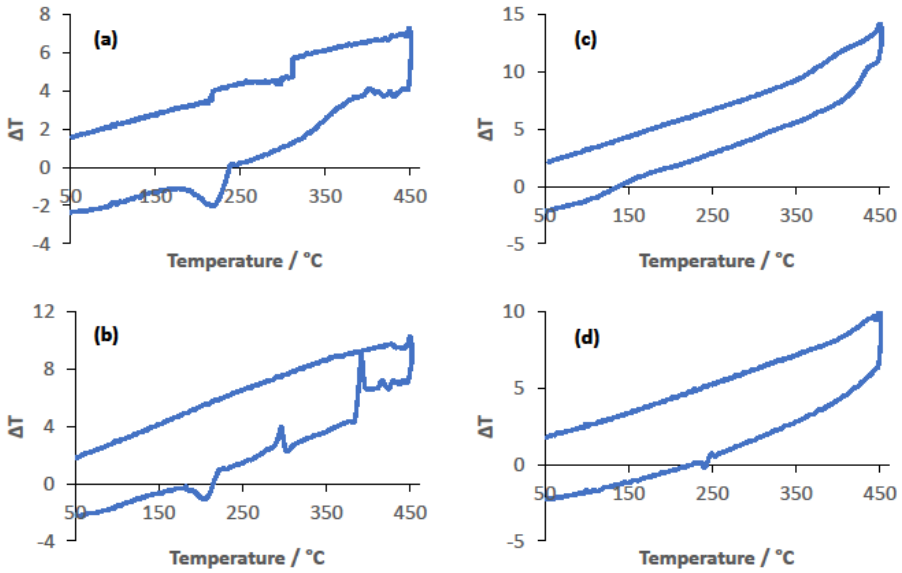

482

483 Figure 6: MWTA plots obtained for picolinate compounds. (a) magnesium picolinate, (b) calcium
484 picolinate, (c) strontium picolinate and (d) barium picolinate.

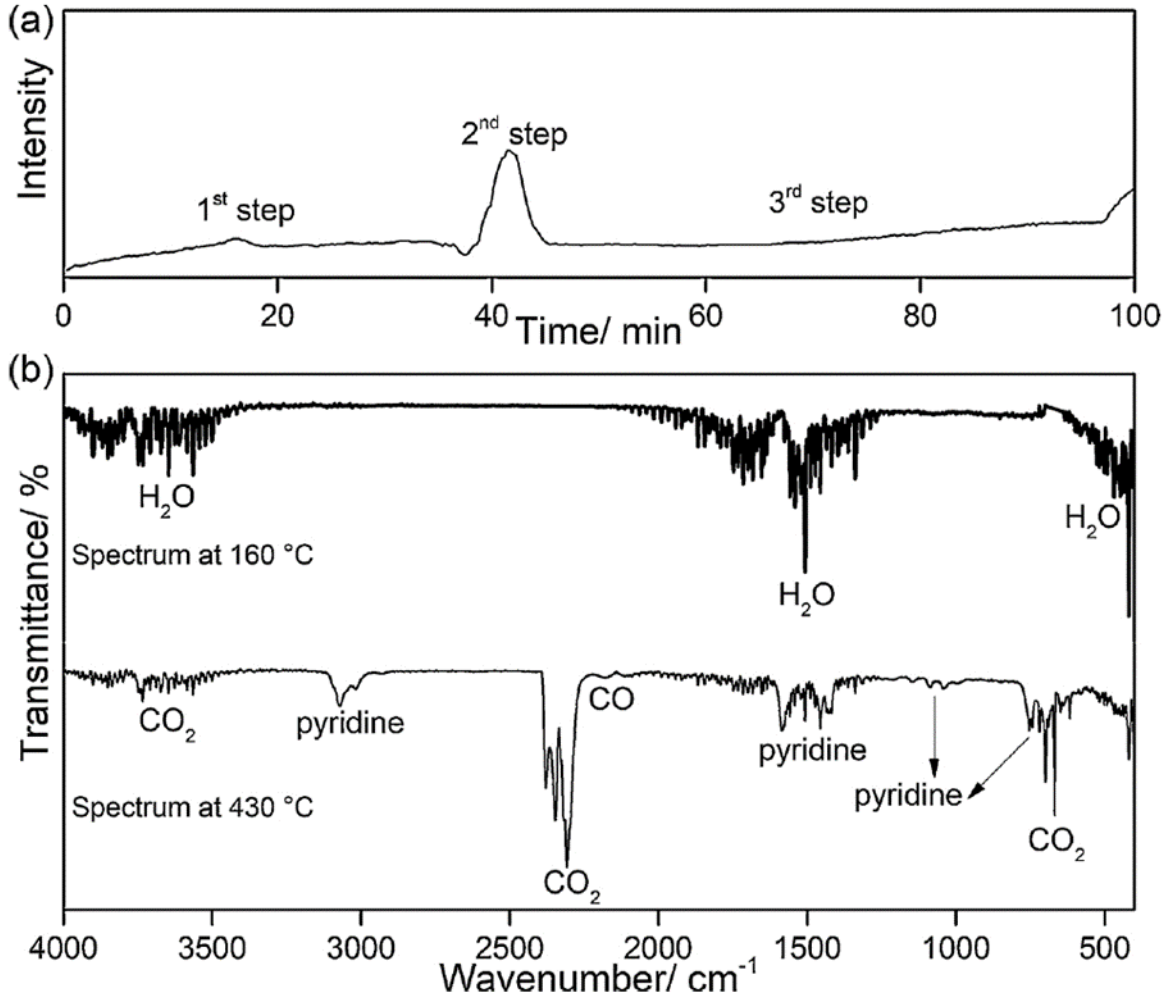

485

486 Figure 7: (a) Gram–Schmidt curve in nitrogen atmosphere; (b) IR spectra of gaseous products evolved
487 during the decomposition of the magnesium picolinate.

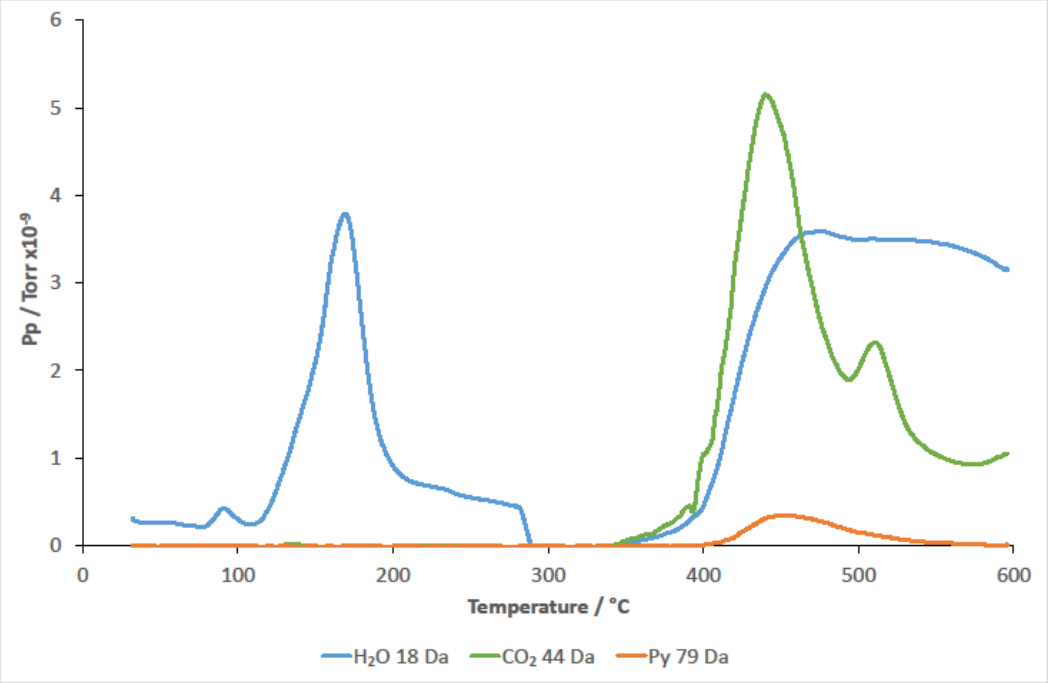

Figure 8: Mass spectra of the gaseous products evolved during the thermal decomposition of magnesium compound in helium atmosphere.

Table 1
Analytical and thermoanalytical (TG[a]) data for $M(L)_2 \cdot nH_2O$ compounds.

Compounds	Metal oxide/ %			L (Lost)/ %		Water/ %		C/ %		N/ %		H/ %		Final Residue
	Calc.	TG	EDTA	Calc.	TG	Calc.	TG	Calc.	EA	Calc.	EA	Calc.	EA	
$Mg(L)_2 \cdot 2H_2O$	13.39	13.15	13.26	75.09	74.40	11.76	12.27	53.67	52.90	10.43	10.42	4.51	4.29	MgO
$Ca(L)_2 \cdot 1H_2O$	18.41	18.45	18.48	75.67	75.32	5.92	6.23	47.67	48.02	9.27	9.38	3.34	3.11	CaO
$Sr(L)_2 \cdot 1.5H_2O$	28.71	28.73	28.68	63.80	63.87	7.49	7.11	40.16	40.50	7.81	7.60	3.10	3.50	SrO
$Ba(L)_2$	50.27	50.66	50.60	48.55	48.12	–	–	36.90	37.15	7.17	7.31	1.96	2.11	$BaCO_3$

[a] TG in air atmosphere, L = picolinate.